Proceedings of the IASS Annual Symposium 2019 — Structural Membranes 2019
Form and Force
7—10 October 2019, Barcelona, Spain
C. Lázaro, K.-U. Bletzinger, E. Oñate (eds.)

X-Shell Pavilion: A Deployable Elastic Rod Structure

Florin ISVORANU*, Julian PANETTA, Tian CHEN, Etienne BOULEAU[a], Mark PAULY

* LGG-EPFL
Lausanne, Switzerland
florin.isvoranu@epfl.ch

[a] INGENI SA Geneve

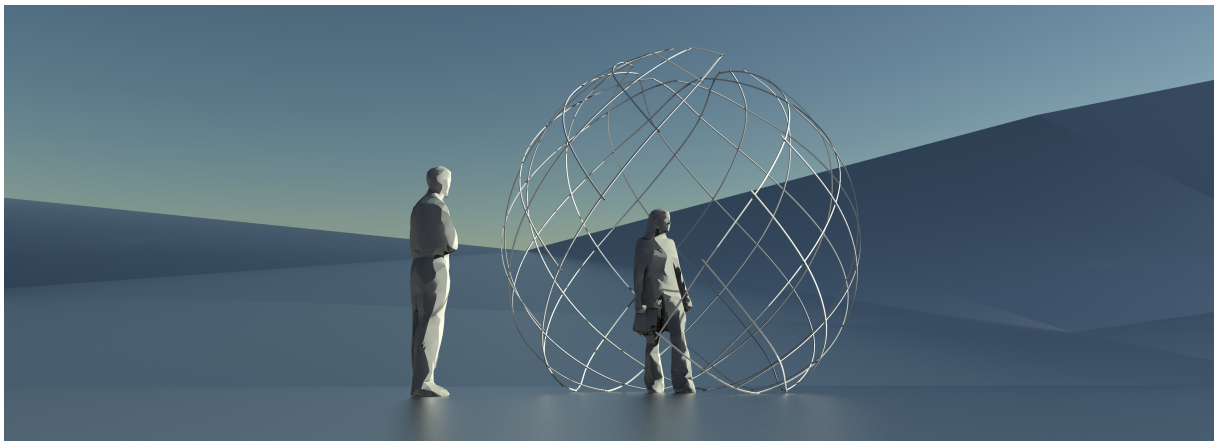

Figure 1: The X-Shell pavilion.

Abstract

We present the X-Shell pavilion, a lightweight structure composed of elastic beam elements joined in a special layout that allows easy on-site deployment. The structure's undeployed assembly configuration lies mostly flat and is easy to build, consisting of GFRP rods connected with mechanical fasteners made of aluminum and steel. The structure is deployed simply by either stretching the flat layout or by driving open the angles between rods at the joints. As the structure expands, the constraints imposed by the joints force its beams to bend and the whole structure buckles into its predetermined target shape. Unlike traditional gridshells, our structure does not require boundary supports to maintain its shape. Instead, the structure's shape is directly encoded in the flat layout of its beams, their cross-section geometry, and material properties. The structure can be locked in its deployed configuration just by fixing a few joints. Apart from simplifying deployment, this feature offers several advantages. For instance, it allows the beam ends touching the ground to be mounted on castor wheels without the structure collapsing back into its flat state.

Keywords: Gridshells, deployable structures, physics-based simulation, numerical optimization, computational design.

1 Introduction

1.1 Concept

X-Shells define a new type of deployable beam structures [2, 1]. They are formed by elastic rods connected in a grid-like network similar to traditional elastic gridshells, but with specific properties that clearly set them apart. The network is assembled in a very compact, usually flat state by connecting beams with rotational hinge joints alternating beams in a scissor type mechanism. The distance between the joints along the beams is non-uniform. As a consequence, the beam network defines an *incompatible* planar linkage mechanism that, when expanded, causes the beams to bend and twist and the entire structure to buckle out of plane towards the desired double-curved target shape.

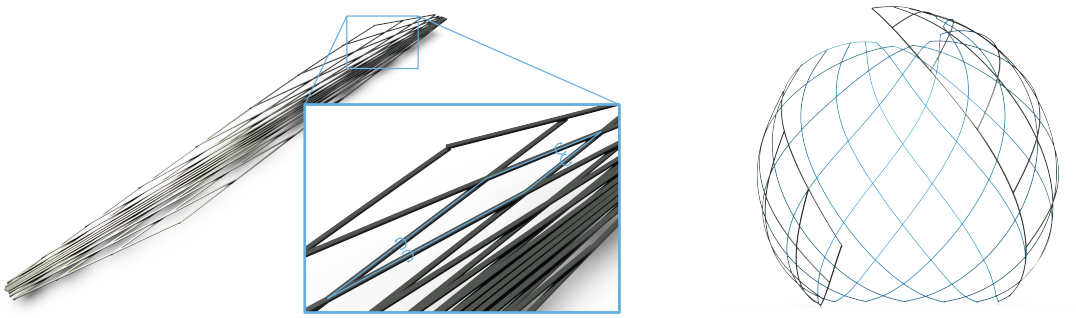

Figure 2: The X-Shell concept: a flat assembly of beams coupled with rotation joints (left, zoomed view) forms an incompatible linkage mechanism that buckles into a programmed 3d shape (right) when deployed by an expansive actuation.

As a new class of gridshell structures, X-Shells do not require any boundary anchors to reach and keep the target shape. Due to the complex interaction between discrete joints and continuously deforming beams, not every X-Shell mechanism is easily deployable or usable architecturally. Exploring the shape space is a challenge requiring specialized simulation and optimization tools.

1.2 Design Tools

We have proposed new computational tools to simulate and optimize X-Shells based on a discrete rod model that allows effective shape exploration [2]. This robust algorithm is complemented with a method for finding sparse actuation layouts in order to efficiently deploy an X-Shell from its compact assembly state to its 3D target state.
The current workflow is limited to forward simulation, although our optimization framework enables the possibility to fit to a reference surface if a good initialization is provided. The design process involves feeding the simulation algorithm with a user generated network of rods, their material properties, and cross-section profile. The tool can then deploy the X-Shell through a range of opening angles with real-time visual feedback. A numerical optimization is applied to optimize the geometry of the deployed and undeployed state. This optimization not only improves the visual quality of the X-Shell, but, more importantly, reduces high local stresses in the structure to ensure easy fabrication and deployment. For details on the algorithms and interfaces used for the design and optimization of the X-Shell pavilion, please refer to [2].

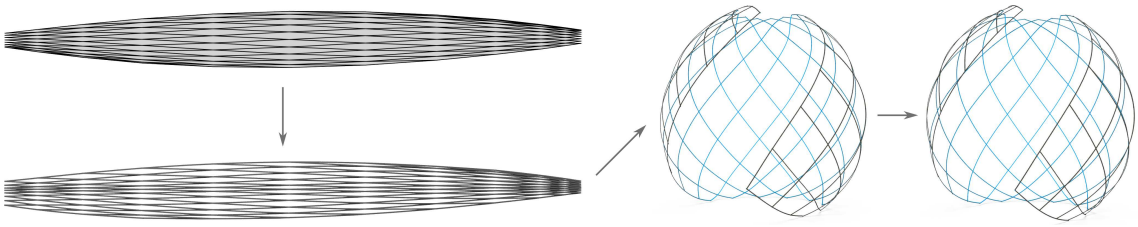

Figure 3: Design pipeline for X-Shells. Our X-Shell simulation framework converts the user-generated rod layout network (upper left) into a coupled assembly of discrete elastic rods and computes its equilibrium in the absence of actuation forces (bottom left). The simulation then drives open the joint angles to obtain the deployed shape (middle), and once the user is happy with the shape, an optimization pass is run to find a nearby X-Shell design with better stress performance (right).

2 Design

2.1 Goals and Constraints

X-Shells are particularly suitable for building temporary lightweight structures. To demonstrate their advantages, we set out to design and build an X-Shell pavilion within a highly constrained design space set out in the Form and Force 2019 pavilion competition: The pavilion bounding box should not exceed 4m × 4m × 4m; it must be self-standing without the need for ground or suspended anchors, but it can be ballasted for stability; it must be transportable, fitting in a maximum of 6 1m × 0.75m × 0.65m cases weighing no more than 32kg; it must be erected/dismantled in one day; and aesthetically, it should reflect the underlying state of the art research and be a pleasant attraction.

2.2 Architectural Typology

The X-Shells design space is quite rich, enabling elegant canopies, intriguing dynamic structures, or biologically inspired shapes. For this particular pavilion project, we are interested in harvesting the purity of their geometric and physical expression, seeking unifying shapes that flow smoothly, integrating wall supports and ceiling into a monocoque structure. Our initial study identified six potential candidates, shown in Figure 4. We settled on the candidate on the lower right as it showcases the free boundaries that distinguish X-shells from conventional elastic gridshells. We also found the design appealing in how it wraps around and embraces its interior during deployment.

3 Construction

X-Shells are easy to build, and from our experiments so far, they are tolerant to construction imprecision. We chose unidirectional GFRP profiles with rectangular 12mm × 8mm cross-sections for the pavilion's beams, based on their properties and availability. The hinge joints employ 3mm diameter 12.9 grade bolts. The connecting sleeves are two-part machined aluminum plates. The bounding box of the deployed X-Shell is 3.2m × 3.2m × 3.6m.

For precise positioning, we laser etched drilling locations and cutting guides directly on the GFRP rods. We then drilled the beams using a bench top drill press aided by a laser cut jig to improve hole alignment (Figure 5) and cut the rods along the etched guides with a band saw.

The X-Shell pavilion is assembled in its flat, low energy state, by pinning corresponding rods until the lattice is complete. While this assembly state has low energy, the energy is not zero: all

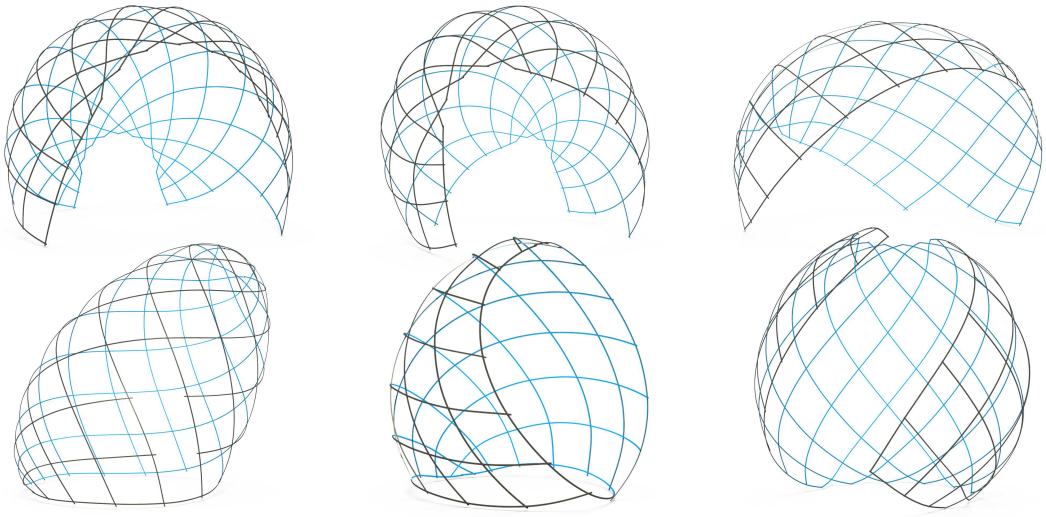

Figure 4: X-Shell pavilion design candidates.

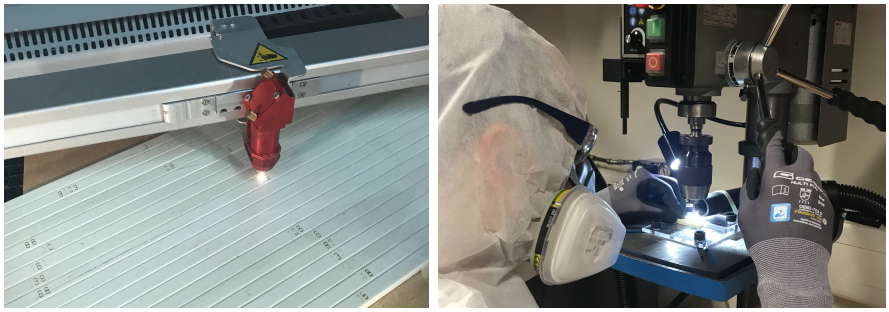

Figure 5: Etching and drilling the GFRP rods.

beams must still incorporate some bending. However, due to the chosen sectional profile of the rods, this compact state remains truly flat. The amount of bending required for the assembly is low enough that it can be manually assembled without power tools, jigs or additional supports. We note that using cross-sections with a higher horizontal aspect ratio could cause the assembly to pop out of plane into a mildly bent shape.

4 Deployment

As an X-Shell mechanism, the pavilion deploys to its designed form from a compact, flat assembly state. Furthermore, to increase transportability, it can be decomposed into shorter, pre-assembled flat sections that join into each other with simple sleeve joints.
Once fully assembled, the pavilion is deployed into the full 3D form by driving open a few of its joint angles, either mechanically or by hand. The X-Shell pavilion can be locked in the deployed state by restricting the lengthening of short quadrangle diagonals using soft stays that clip onto the respective quadrangle joints. Only a few stays suffice to lock the structure open.

Figure 6: Assembly and deployment of the X-Shell pavilion. The aluminum connecting sleeves (upper left) are used to join the separately-assembled scissor linkages of GFRP beams into the full assembly (bottom left, middle). A preliminary manual deployment (right).

5 Performance

We judge the X-Shell pavilion's performance mainly from a structural point of view. Since X-Shells behave as mechanisms, we are interested in analyzing their load behavior and displacements in the deployed state while in the flat (undeployed) and intermediary states we need to assess the internal stresses that could possibly lead to node failure and rod breakage or require excessive deployment forces. Figure 7 plots the pavilion's stress throughout its entire deployment as predicted by our simulation framework. We note that our X-Shell optimization tool is able to substantially reduce the stresses due to beam bending even though the initial design candidate found by forward exploration was already free of any obvious design flaws.

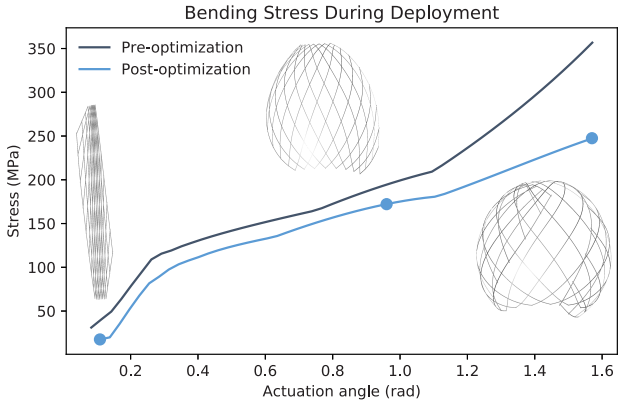

Figure 7: Maximum stresses in the optimized and unoptimized X-shells due to beam bending throughout the deployment process. The inset renderings visualize the deployment stages indicated by the blue disks.

We conducted our analyses using the X-Shell simulation framework [2] to simulate deployment and an Abaqus model for static loading. The current simulation framework and the Abaqus model ignore the drill holes in the rods at the joints. To analyze the structural consequences of the piercings, we separately conducted destructive tests of the rod joints with various piercing sizes and loads; these showed a pin size of 3mm satisfies structural requirements, considering the loads encountered in the X-Shell deployment.

5.1 Experimental Testing

To calibrate our deployment simulations with accurate material parameters and predict the structural integrity of the deployed X-Shell, we conducted four sets of experiments assessing the structural behavior of the GFRP, the sleeve connectors, and the capacity of the joints.

Four point bending along the weak axis of GFRP to derive the Young's modulus. We determined the Young's modulus of the GFRP beams using a four point bending experiment performed on a static load testing machine (Instron 5940 Series Universal Testing Systems) with a load cell capacity of 1kN. A force based loading is imposed at a rate of $1\frac{\text{N}}{\text{s}}$. Rollers are used both at the supports and at the points of load application. The reaction forces and displacements are recorded at 10Hz.

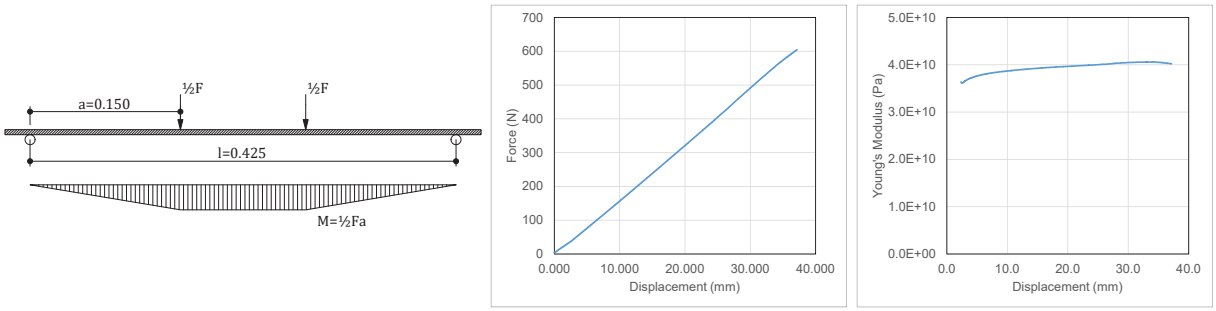

Figure 8: Force/displacement of GFRP under four point bending (left); derived Young's modulus (right).

The resulting force/displacement curve shows a linear relationship for the range of force tested (Figure 8). The analytical solution for the Euler-Bernoulli beam equation under the four-point bending boundary conditions gives us an expression for the displacement at $x = (a = 0.150\text{m})$ under a given force magnitude which can be rearranged to obtain the Young's modulus: $E = \frac{Fa^2}{12dI}(3l - 4a)$, where $l = 0.425\text{m}$, I is the second moment of area, F is the applied force, and d is the downward displacement. Each (F, d) measurement gives us a different estimate of E, as plotted in Figure 8, and we chose $E = 4 \times 10^{10}\text{Pa}$ for use in our simulations.

Four point bending along the weak axis of GFRP with a sleeve connector. We assessed the difference in stress-strain behavior between a simple section and one with a sleeve connector using a second four point bending test. Surprisingly, their bending stiffnesses are virtually indistinguishable (Figure 9), implying that decomposing the X-Shell's beams into segments to satisfy our transportability constraints will not significantly affect the deployed structure's shape or load behavior.

Testing the bolt capacity and delamination. We investigated the potential for local delamination in the direction perpendicular to the fibers. Two beams are connected using a stainless steel M4 bolt with a washer in between. Load up to 550N is applied in compression with no visible failure in either the bolt or the laminates.

Three point bending along the strong axis to obtain material strength. We measured the tensile strength of the GFRP beams by conducting a three point bending experiment

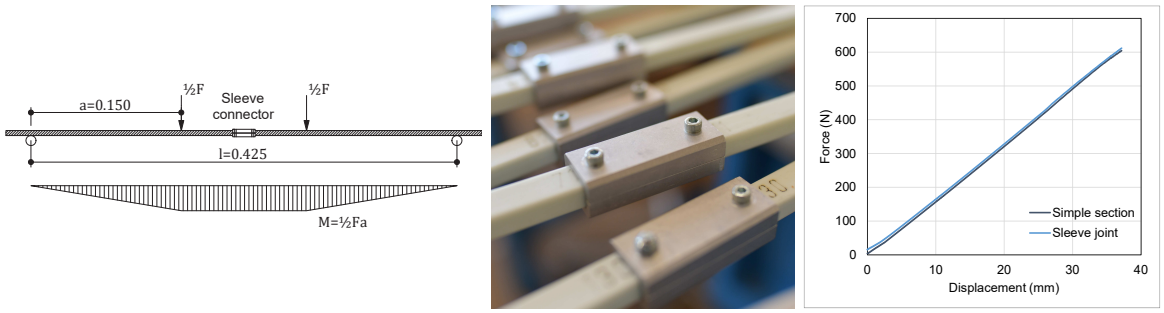

Figure 9: A sleeve connector (left) and the four point bending force displacement plot comparing the bending stiffness of a single GFRP beam to two GFRP beams joined with a sleeve connector (right).

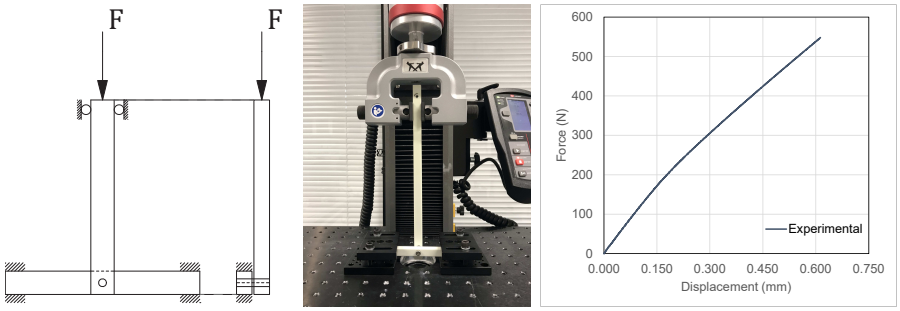

Figure 10: Experimental setup for testing the bolt capacity (left) and results (right).

inducing a large mid span stress at the extremities of the cross section. We used the strong axis to reduce the necessary clearance for deflection. The corresponding analytical solution to the beam equation yields the following expression for the greatest maximum principal stress in the cross-section: $\sigma = \frac{My}{I} = \frac{1}{2}Fl\frac{h}{2}\Big/\frac{bh^3}{12}$.

This linear elasticity-based model agrees with the initial slope of the stress strain curve (Figure 11), but as damage accumulates, the behavior becomes non-linear and the beam fails at approximately 0.014 strain with rupture of fibers on the tension side. The maximum stress reached is conservatively 400MPa. This stress limit is compared with the detailed simulations in the next section to ensure that our design has an adequate safety factor.

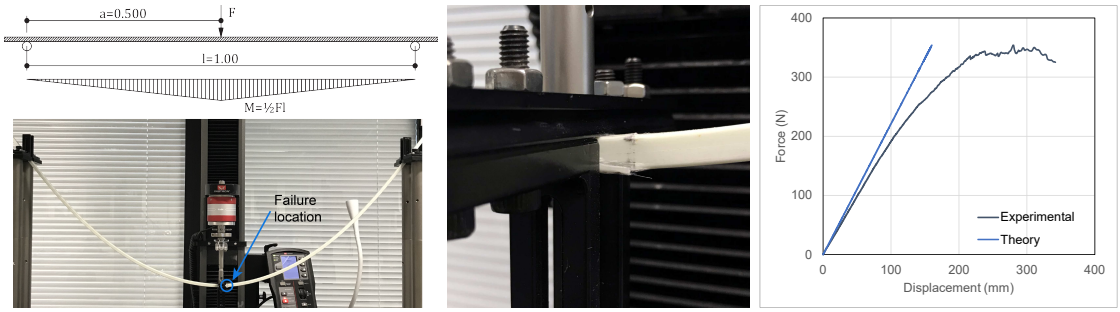

Figure 11: Three point bending experiment inducing failure at mid span (left) with a detailed view (center). The stress strain curve of resulting from the experiment in comparison with theoretical prediction.

6 Detailed Finite Element Simulations

The X-Shells simulation framework [2] does not capture the beam behavior when the cross section has defects such as bolt holes. We perform solid FEA to simulate isolated segments of the deployed structure to demonstrate that the maximum stress remains below the limit in such disturbed regions. As it is unclear where the absolute maximum principal stress will occur within the structure, four different segments are chosen for detailed analysis: the regions of maximum bending stress, twisting stress, joint force, and joint torque (Figure 12).

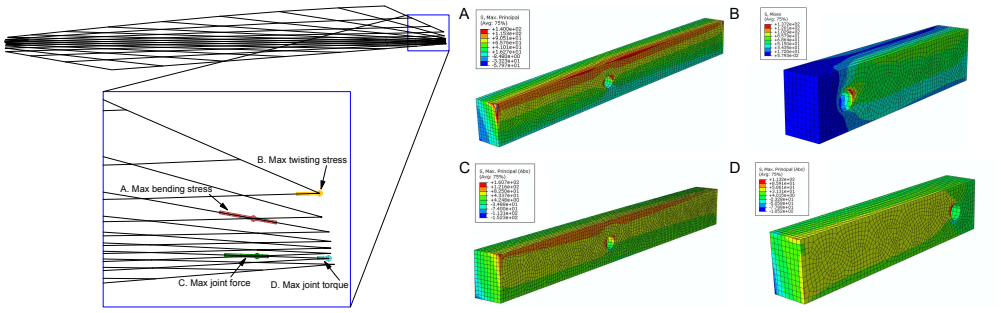

Figure 12: Critical members and their maximum principal stresses computed by Abaqus.

We used Abaqus 14 to simulate the structural behavior using quadratic hexahedral elements. We extracted equivalent forces and torques acting on the segment in question from the X-Shells deployment simulation and applied them to reference points placed at the segment ends and bolt hole centers. These reference points are in turn coupled (in all 6 DOFs) to the faces at the ends of the segment, and to the cylindrical surface made by the bolt hole. To eliminate rigid body motion, one set of forces and torques is replaced by a clamped boundary condition. The cross section is 12mm × 8mm, and the Young's modulus is set at 40 000MPa.
We found stresses concentrate at the rims of the bolt holes and along extreme edges of the cross section. For beam segments on the X-shell boundary, maximum stress occurs only at the bolt holes. We observe an approximate peak stress of 130MPa which offers a safety factor of roughly 3 compared to the experimental capacity of 400MPa.

7 Conclusion

X-Shells are generally easy to build and deploy. Compared to traditional regular elastic gridshells, they have two significant advantages: they do not rely on boundary anchors to develop into the designed shape; and their freedom to eschew boundary constraints enables a much richer design space. These particular advantages make X-Shells highly suitable for mobile and immobile architecture at small and medium scale: pavilions, shelters, concert installations, temporary roof structures, re-configurable domes and canopies.

References

[1] Bouleau, E., Panetta, J., Isvoranu, F., and Pauly, M. X-shell, a new spatial deployable lattice compared to traditional reticulated shells. In *Form and Force 2019: Proceedings of the IASS Annual Symposium 2019* (2019).

[2] Panetta, J., Konaković-Luković, M., Isvoranu, F., Bouleau, E., and Pauly, M. X-shells: A new class of deployable beam structures. *ACM Trans. Graph. 38*, 4 (July 2019).